

## Original Article

# Protective effects of astaxanthin against diabetic retinal vessels and pro-inflammatory cytokine synthesis

Ming Yang<sup>1,3</sup>, Tong Zhao<sup>1</sup>, Tingting Deng<sup>2</sup>, Zhijun Wang<sup>1</sup>

Departments of <sup>1</sup>Ophthalmology, <sup>2</sup>Institute of Clinical Medical Sciences, China-Japan Friendship Hospital, Chaoyang District, Beijing, China; <sup>3</sup>Peking Union Medical College, Dongcheng District, Beijing, China

Received February 22, 2018; Accepted June 29, 2018; Epub May 15, 2019; Published May 30, 2019

**Abstract:** Background: Diabetic retinopathy (DR) is a common microvascular complication of diabetes and a leading cause of blindness. Astaxanthin (AST) is a naturally occurring carotenoid with many biological protective activities. The purpose of the present study was to investigate the protective effects of AST on DR in a rat model of type 1 diabetes mellitus (DM) and to examine the mechanisms involved. Methods: An intraperitoneal injection of 1% streptozotocin was used to prepare the rat model of diabetes. Rats were randomly assigned to one of three groups: untreated control, diabetes + olive oil (DM), or DM+AST (n = 8 per group). The AST group received 20 mg/kg/day AST dissolved in olive oil by gavage. The DM group received an equal volume of olive oil. During the study, blood glucose levels and body weights were measured every two weeks. After six months, retinas were excised to prepare the retinal capillary network. Endothelial cell to pericyte ratio (E/P) and the numbers of acellular capillary strands were compared among different experimental groups. Formation of advanced glycation end products (AGEs) and expression of interleukin-6 (IL-6), tumour necrosis factor- $\alpha$  (TNF- $\alpha$ ), and caspase-3 in retinal tissues were assessed by immunohistochemistry and RT-PCR. Results: AST slightly increased body weight but had no significant effects on blood glucose levels. E/P and numbers of acellular strands in the DM+AST group were lower than those in the DM group. Expression of AGE, IL-6, TNF- $\alpha$ , and caspase-3 in retinal tissues decreased compared with those of the DM group. All differences between the groups were statistically significant ( $P < 0.05$ ). Conclusion: AST can protect pericytes from apoptosis and delay development and progression of DR in streptozotocin-induced diabetic rats. Additionally, it can reduce generation of AGEs, release of inflammatory cytokines (IL-6, TNF- $\alpha$ ), and cleavage of caspase-3, which may mediate pericyte apoptosis.

**Keywords:** Astaxanthin, diabetic retinopathy, anti-apoptosis, anti-inflammation

## Introduction

Diabetes is a systemic metabolic disease characterized by chronic hyperglycaemia. The retina is one of the most vulnerable tissues [1-3]. Diabetic retinopathy (DR) is the most common microvascular complication of diabetes, known to be the leading cause of blindness [4]. DR is characterized by progressive retinal vasculopathy, leading to breakdown of the blood-retina barrier (BRB), leakage of retinal vessels, oedema, ischaemia, and neovascularization [5]. Mechanisms of the development of DR are not fully understood, but some distinct biochemical pathways have been associated with development of DR, including pericyte apoptosis, advanced glycation end-product (AGE) formation, oxidative stress, and inflammation [6]. Therefore, researchers have focused on meth-

ods to delay progression of DR by inhibiting pericyte apoptosis and reducing accumulation of AGEs and inflammatory response [7, 8].

Astaxanthin (3,3'-dihydroxy- $\beta,\beta'$ -carotene-4,4'-dione, AST) is a naturally occurring carotenoid reported to have a wide variety of biological functions, including anti-inflammatory, anti-apoptosis, antioxidant (10 times higher than that of other carotenoids), anti-cancer, and neuroprotective effects [9-11]. The study of AST has received increasing attention. AST has been reported to have the capacity to reduce inflammation and apoptosis [12]. In a study conducted by Dong et al., treating cultured RGC-5 ganglion cells with astaxanthin decreased hydrogen peroxide-induced apoptosis in the control group. However, molecular mechanisms by which AST inhibits apoptosis of peri-

# Astaxanthin against diabetic retinal vessels and inflammatory

cytes in streptozotocin (STZ)-induced diabetic rats remain unclear [13].

The present study evaluated the protective effects of AST in a rat model of type 1 diabetes mellitus (DM) by determining its effects on general symptoms of DR, pericytes, inflammatory response in the retina, and retinal vessel damage.

## Materials and methods

### *Animals*

Twenty four male Sprague-Dawley rats, aged 6 weeks and weighting 260-280 g, were purchased from Beijing HFK Bioscience Co. Ltd. (SCXK (Jing) 2014-0005). The animals were kept in an ordinary housing facility in keeping with national standards (Laboratory Animal Requirements of Environment and Housing Facilities [GB 14925-2001]). All experimental procedures were performed according to the ARVO statement for Use of Animals in Ophthalmic and Vision Research.

Animals were fed and housed in the center and maintained under conditions of controlled temperature (20-24°C), relative humidity of 40%, and a 12-hour light-dark cycle. All rats had free access to food and water throughout the study. Bedding was changed daily and the rats were monitored regularly.

### *Experimental procedure*

The animals were fasted for 12 hours prior to establishing the diabetic model. Rats in the DM groups were injected intraperitoneally with 1% STZ (Sigma-Aldrich, St. Louis, MO, USA) and dissolved in citrate buffer (pH 4.5) at 60 mg/kg. Rats in the negative control group received the same volume of citrate buffer only. A blood glucose level > 16.7 mmol/L for three consecutive days indicated successful establishment of the DM model. Treatment with AST (Sigma-Aldrich, St. Louis, MO, USA) was started 3 days after diabetes confirmation and continued for 24 weeks. Dosage (in mg/kg) was calculated with the formula given below: Dosage of AST = Minimum Inhibitory Concentration × 20 [14].

The animals were allocated randomly to three groups of eight animals each: [Control group], C: normal rats received 0.9% NaCl by daily gavage and served as a negative control gr-

oup. [Diabetic group], DM: diabetic rats received olive oil by gavage each morning. [Diabetic + AST-treated group], DM+AST: diabetic rats received AST (20 mg/kg/day) in olive oil by gavage each morning.

During the experimental period, all rats had free access to food and water. Blood glucose levels and body weight were measured every 2 weeks. At the end of the study, the rats were euthanized with an overdose of chloral hydrate anaesthesia. Eye globes were immediately removed, weighed, marked, and stored at -80°C until analysis.

### *Retinal capillary network preparation*

Eye globes were placed in 4% paraformaldehyde for 72 hours. The cornea and lens were then removed under a microscope. The retina was separated from the choroid carefully using a blunt metal spatula. The optic nerve was removed with scissors, carefully, to not damage the retina. The intact retina was divided into four pieces and they were then put in a test tube with trypsin solution (3% in sodium phosphate buffer, pH 7.2-7.4). The retina was digested for 3 hours in a water bath at 37°C, mixing 3-4 times during the digestion. The inner limiting membrane was peeled away and a cat's whisker was used to clear the remaining nerve tissue on the retinal vascular network under a microscope. Tissue pieces were placed on a slide and allowed to air-dry. After periodic acid-Schiff (PAS) staining, retinal capillary cells (pericytes) were counted across five views of the central area (400 × magnification) under a microscope. Endothelial/pericyte (E/P) ratio was calculated and compared between the different experimental groups. Numbers of acellular collapsed capillary strands were also counted in five views (400 × magnification) per retina.

### *Immunohistochemical staining*

Eyeballs were fixed in 4% paraformaldehyde for 3 days (Sigma-Aldrich, St. Louis, MO, USA), placed vertically in tissue cassettes, and paraffin-embedded. After deparaffinization and rehydration, sections were stained with haematoxylin and eosin for examination of pathological changes in morphology. To visualise cytokines, sections were first incubated with 0.1% hydrogen peroxide in phosphate-buffered saline (PBS) for 30 minutes to block the activity of

**Table 1.** PCR primer sequences and amplified product sizes

Gene	Primer sequence (5'-3')	Product size (bp)
RAGE	AGCCTTGCTGAACCTCTTCT	92
	GGTTCAGGTAGCCAAACCAT	
IL-6	ATGAACAGCGATGATGCACT	135
	ACGGAAGCTCCAGAAGACCAG	
TNF- $\alpha$	GACCAGCCAGGAGGGAGAAC	127
	TCCGGAGGGAGATGTGTTGC	
Caspase-3	GCACACGGGACTTGAAAGC	112
	AGGAAGCCTGGAGCACAGAC	

Abbreviations: AGE, advanced glycation end products; IL-6, interleukin-6; TNF- $\alpha$ , tumour necrosis factor- $\alpha$ .

endogenous peroxidases. After washing three times with PBS, sections were blocked with 10% goat serum at 37°C for 30 minutes and then incubated with rabbit anti-rat AGE (1:100), IL-6 (1:100), TNF- $\alpha$  (1:100), and cleaved caspase-3 (1:100) primary antibodies (Sigma-Aldrich, St. Louis, MO, USA) at 4°C for 24 hours. After washing, sections were then incubated with species-appropriate horseradish peroxidase-conjugated secondary antibodies (Sigma) for 30 minutes at 37°C. Slides were washed three times with PBS and stained with 3,3'-diaminobenzidine (DAB, Zhongshan Golden Bridge Biotechnology, Beijing, China). A positive signal in the retina was brown. Five visual fields of each section were selected randomly (400 × magnification), captured, and integrated optical density (IOD) was calculated using Image-Plus 6 image analysis.

#### Real-time PCR

Left posterior segments were put in a Petri dish filled with distilled water. The retina was removed from the pigment epithelium under a dissecting microscope for preparation of total RNA. Total RNA was extracted from the retinas with TRIzol™ Reagent (Invitrogen, Carlsbad, CA, USA). Reverse-transcriptase PCR was used to measure mRNA levels of RAGE, IL-6, TNF- $\alpha$ , and caspase-3 in retinal tissue. Concentration and purity of total RNA was measured using an ultraviolet spectrophotometer (Takara, Shiga). Oligonucleotides were used as primers in a 25- $\mu$ L reaction system (Takara). Oligo sequences are shown in **Table 1**. Moloney murine leukaemia virus reverse transcriptase (M = MLV RT) was used to synthesize cDNA (Takara). RT-PCR Master Mix (GoTaq®, Promega, Madison, WI, USA)

was used for amplification and a LightCycler® 480 system (Roche Diagnostics Corporation, Indianapolis, IN, USA) was used for detection. After completion of the reaction, the threshold cycle value (Ct) for all curves was calculated. Using a base of two, the difference in exponents of the values obtained was used to calculate relative expression of the target genes. Each experiment was performed with three or more replicates. The melting curve of PCR products showed a single peak. Agarose gel electrophoresis was used for further verification of product size.

#### Statistical analysis

Data are expressed as mean  $\pm$  standard deviation (SD). Student's t-tests and one-way analysis of variance (ANOVA) with Tukey's multiple comparison testing were used in Prism 5.0 software (GraphPad Software Inc., San Diego, CA, USA) to compare differences between groups. Differences with  $P < 0.05$  are considered statistically significant.

## Results

### Body weight and blood glucose

Body weight and blood glucose measurements are shown in **Figure 1**. Initial body weights were similar in all groups, but final body weights were lower in the diabetic rats than in control rats. Average body weight in the DM+AST group was higher than that of the DM group at all time points (**Figure 1A**). As expected, injection of STZ increased blood glucose levels after 24 weeks, but there were no statistically significant differences in blood glucose levels between the DM groups with or without AST (**Figure 1B**).

### PAS staining of retinal vessel preparations

Results of retinal vessel staining are shown in **Figure 2**. Retinal capillary networks are visible at a high magnification. In the C group, the main artery was round, uniform, and strongly stained. The vein was lightly stained and had a large diameter. Capillaries were reasonably straight, of uniform diameter, and interconnected into a network (**Figure 2A, 2D**). At a higher magnification, the capillaries were mainly composed of two types of cells. One cell type was endothelial cells, which had a large, oval, or round nucleus that was stained lightly and was generally locat-

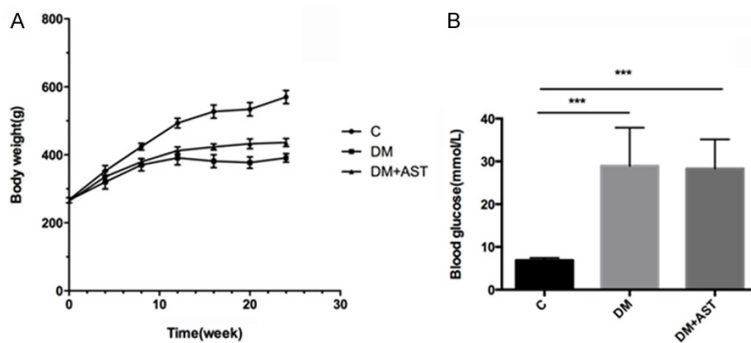


**Figure 1.** Body weights and blood glucose levels in study groups at different time points. A. Body weights of the rats in each of the three treatment groups, monitored over 24 weeks. B. Blood glucose levels in each of the three treatment groups after 24 weeks. All values are mean  $\pm$  standard deviation ( $n = 8$ ).  $***P < 0.05$  versus the control group. Abbreviations: C, control rats; DM, diabetic rats; DM+AST, diabetic rats receiving astaxanthin.

ed in the central part of the capillary (**Figure 2B**, black arrow). The other cell type was the pericyte, which had a small, round, or triangular nucleus that was stained deeply and was generally located at one side of the capillary wall (**Figure 2A**, black arrow). In the DM group, the retinal arteriovenous trunk and branches appeared tortuous at a low magnification, with capillary network disorder (**Figure 2E**). At a higher magnification, the capillaries had expanded. There were clear indications of local stenosis, kinks in the capillary loops, dense microvascular networks (**Figure 2B**), proliferation of endothelial cells, and pericyte ghosts. The morphology of capillaries in the DM+AST group was between that of the control and DM groups, with reduced vascular tortuosity, dilatation, and stenosis (**Figure 2C**, **2F**).

#### *E/P and acellular capillaries*

As shown in **Figure 3**, the E/P ratio was higher in DM and DM+AST groups than in the C group. Compared with that of the DM group, E/P ratio was lower in the DM+AST group. This difference was statistically significant. Formation of acellular strands was more frequent in diabetic rats than in control rats. Data showed that the number of acellular strands in the DM group was higher than the DM+AST group.

#### *Histological examination and immunohistochemistry of AGEs, inflammatory proteins, and caspase-3 in retinas*

Under low magnification, the structure of each layer of the retina in the C group was clearly

visualized (**Figure 4A**). Inner and outer nuclear layers were clearly visualized. In the DM group (**Figure 4B**), the density of the nuclear layers was reduced, cell arrangement was disorganized, and tissue contained void spaces. In the DM+AST group (**Figure 4C**), the structures of the retina remained intact and the density of the nuclear layers was higher than that of the DM group. This study examined expression of AGEs, IL-6, TNF- $\alpha$ , and cleaved caspase-3 by immunohistochemistry of the retinas (**Figures 5 and 6**). Posi-

tively stained cells were quantified in images. IOD showed higher expression levels of AGEs, IL-6, TNF- $\alpha$ , and cleaved caspase-3 in the retinas of the DM group, compared to those of C and DM+AST groups ( $P < 0.05$ ).

#### *Effects of AST on mRNA levels of RAGE, inflammatory proteins, and caspase-3 in retinas*

The present study observed that there were statistically significant differences between groups in all measured mRNA levels. As shown in **Figure 7**, relative mRNA expression of RAGE, IL-6, TNF- $\alpha$ , and caspase-3 in retinas was quantified. According to results, AGEs, IL-6, TNF- $\alpha$ , and caspase-3 mRNAs were significantly elevated in retinas of the DM group, compared to those of C and DM+AST groups ( $P < 0.05$ ).

#### **Discussion**

Although AST is not naturally present in the human retina, it easily crosses the BRB, subsequently protecting retinal ganglions [15]. However, AST has never been reported to protect pericytes to maintain normal vascular and reduce inflammatory response. For these reasons, it was hypothesized that AST could inhibit pericyte apoptosis by decreasing levels of pro-inflammatory cytokines and pro-apoptotic factors in the retina.

Previous reports have documented that AST can improve diabetic symptoms and delay progression of diabetic complications in experimental diabetes models. These improvements include reducing blood sugar levels, attenuat-

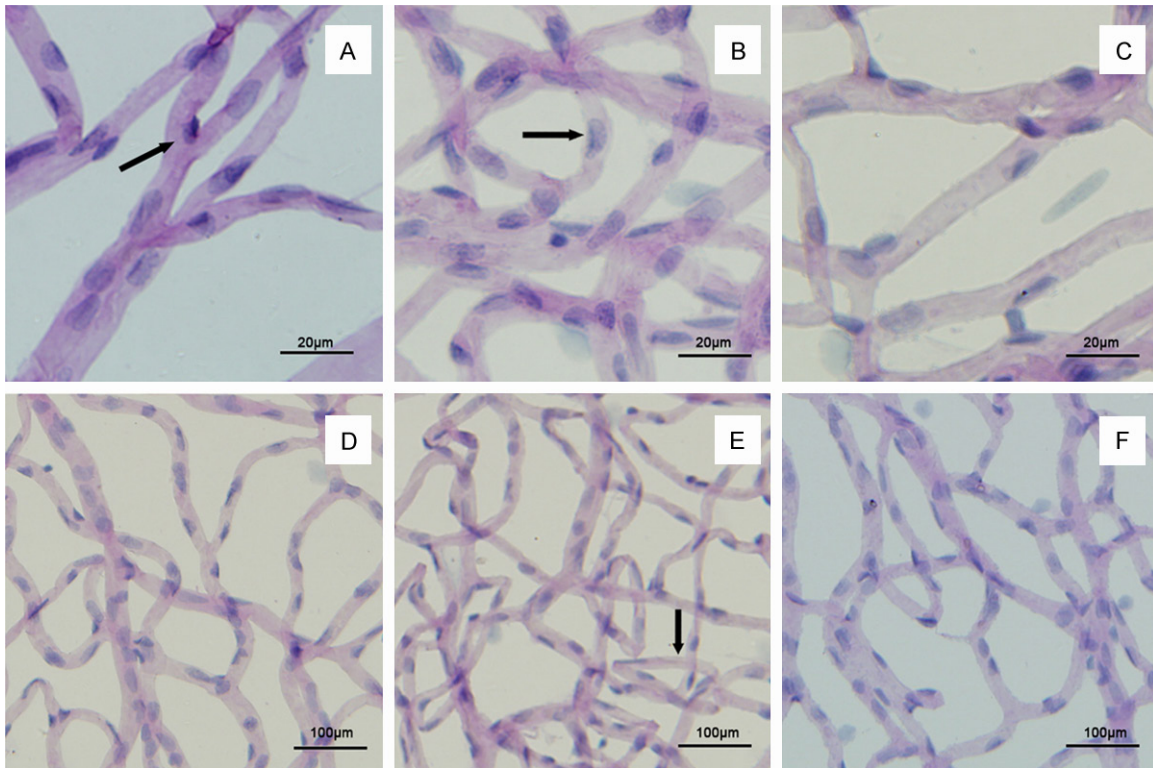


**Figure 2.** Periodic acid-Schiff staining of retinal vessel preparations. A. The normal vessel network of group C (400 × magnification), the arrow shows the pericyte; B. The abnormal vessels of group DM (400 × magnification), the arrow shows endothelial cell; C. The vessel network of group DM+AST (400 × magnification); D. The normal vessels of group C (100 × magnification); E. The abnormal vessel network of group DM (100 × magnification); F. Vessels of group DM+AST (100 × magnification); All images are representative. Abbreviations: C, control rats; DM, diabetic rats; DM+AST, diabetic rats receiving astaxanthin.

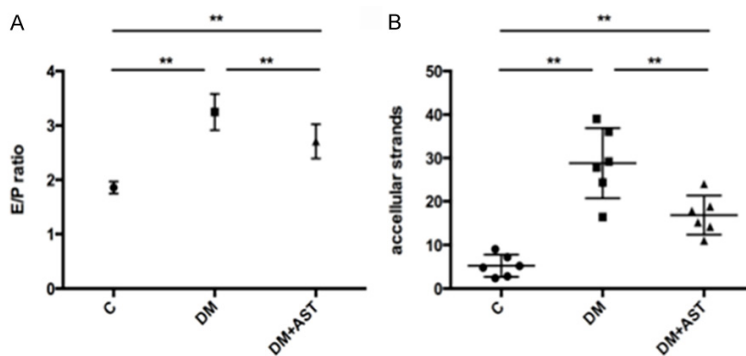


**Figure 3.** E/P ratio and numbers of acellular strands in retinal capillaries. A. E/P ratios of the three treatment groups. Plotted data are mean ± standard deviations (n = 8). B. Number of acellular strands in the three treatment groups. Number of acellular strands counted for each rat is plotted along with the mean and standard deviation of the group. \*\*P < 0.01 for the indicated comparison. Abbreviations: C, control rats; DM, diabetic rats; DM+AST, diabetic rats receiving astaxanthin; E/P, endothelial cell to pericyte ratio.

ing DR, and preventing diabetic nephropathy [12, 13]. Similarly, it was found that AST could partially ameliorate the loss of body weight in diabetic rats. However, present data showed

that blood glucose levels in diabetic rats were not affected by AST treatment, similar to the data of Chan et al. [16].

Retinal capillaries contain endothelial cells, astrocytes, and pericytes. In the inner BRB, endothelial cells are surrounded by pericytes and the foot processes of astrocytes [17]. The main function of pericytes is to maintain vascular stability [18]. Apoptosis of pericytes leads to formation of pericyte ghosts, which increase the numbers of acellular capillaries and proliferation of endothelial cells [19]. Apoptotic cell death alters the retinal structures

and stimulates release of inflammatory mediators [20]. Inner BRB damage results in leakage of retinal vessels, basement membrane thickening, endothelial cell damage, macu-

## Astaxanthin against diabetic retinal vessels and inflammatory

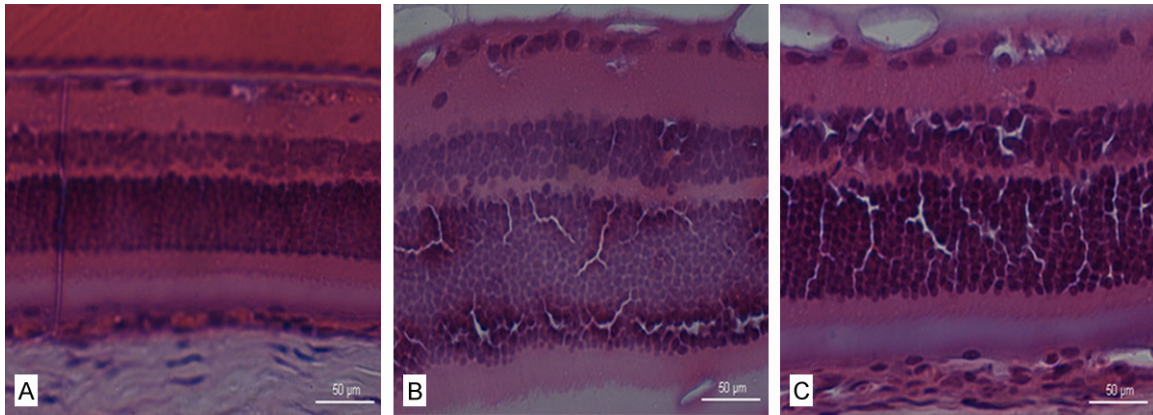


**Figure 4.** Haematoxylin and eosin staining of representative sections of rat retina. A. Group C; B. group DM; C. Group DM+AST. All images are 400 × magnification. Abbreviations: C, control rats; DM, diabetic rats; DM+AST, diabetic rats receiving astaxanthin.

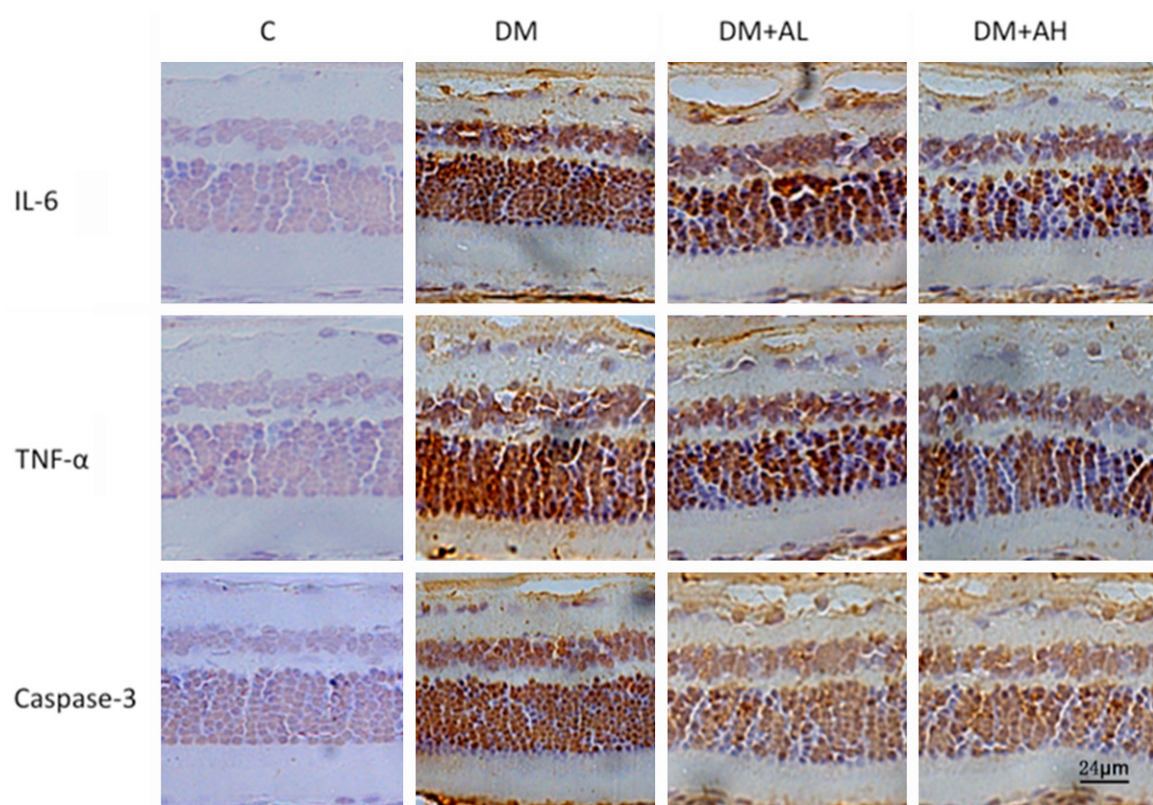


**Figure 5.** Immunohistochemistry of retinal sections (400 × magnification). Positive expression is indicated by dark brown staining. Abbreviations: C, control rats; DM, diabetic rats; DM+AST, diabetic rats receiving astaxanthin; AGE, advanced glycation end products; IL-6, interleukin-6; TNF- $\alpha$ , tumor necrosis factor- $\alpha$ .

lar oedema, and neovascularization [6]. Accumulating evidence has suggested that pericyte apoptosis occurs at an early stage and is a hallmark of DR [21]. However, underlying molecular mechanisms have not been clearly characterized. The present study observed that

rats with diabetes showed higher E/P ratios and greater numbers of acellular capillaries compared to control rats. Data showed that 20 mg/kg AST can decrease the ratio of E/P and numbers of acellular capillaries, compared to those of the DM group. However, ghost cells

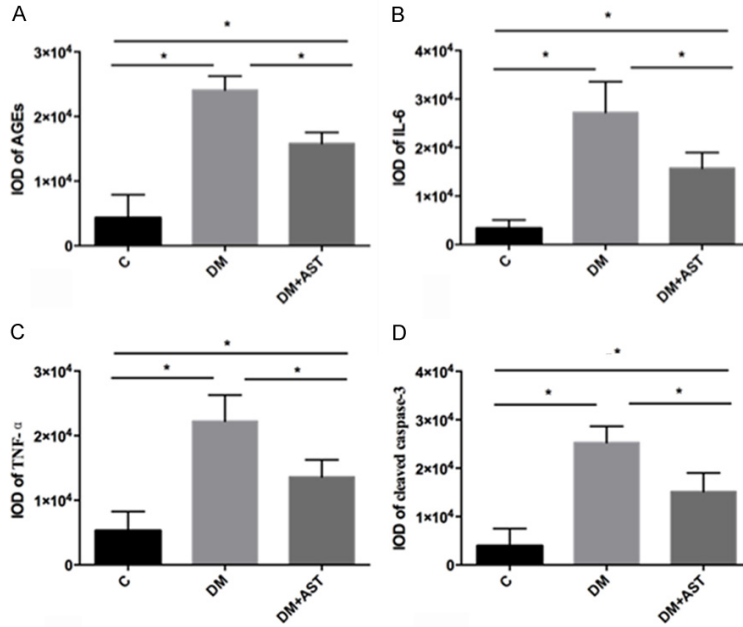


**Figure 6.** Quantification of immunohistochemistry data from **Figure 5**. (A) AGE levels, (B) IL-6 levels, (C) TNF- $\alpha$  levels, (D) Cleaved caspase-3 levels. Expression levels were quantified from immunohistochemistry images, as described in the Methods section. Plotted values are mean  $\pm$  standard deviations ( $n = 8$ ). \* $P < 0.05$  for the indicated comparison. Abbreviations: C, control rats; DM, diabetic rats; DM+AST, diabetic rats receiving astaxanthin; AGE, advanced glycation end products; IL-6, interleukin-6; TNF- $\alpha$ , tumor necrosis factor- $\alpha$ ; IOD, integrated optical density.

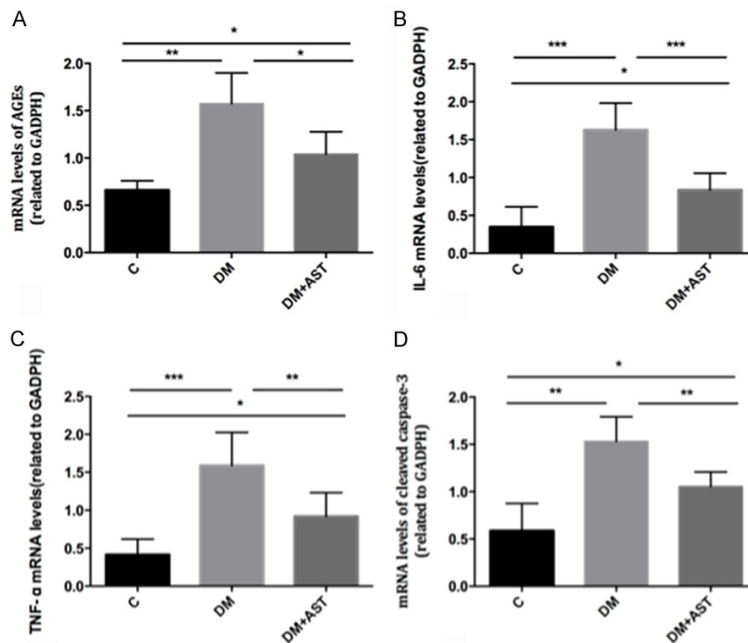


**Figure 7.** Real time reverse-transcriptase PCR of mRNA in the three different treatment groups. (A) Levels of RAGE mRNA, (B) Levels of IL-6 mRNA, (C) Levels of TNF- $\alpha$  mRNA, (D) Levels of caspase-3 mRNA. All values were normalized to that of GAPDH mRNA. Plotted are the means  $\pm$  standard deviations ( $n = 8$ ).  $P < 0.05$ , \*\* $P < 0.01$  and \*\*\* $P < 0.001$  for indicated comparisons.

Abbreviations: C, control rats; DM, diabetic rats; DM+AST, diabetic rats receiving astaxanthin; AGE, advanced glycation end products; IL-6, interleukin-6; TNF- $\alpha$ , tumor necrosis factor- $\alpha$ ; GAPDH, glyceraldehyde 3-phosphate dehydrogenase.

and acellular capillaries were present in both DM and DM+AST groups. In another study, Robison et al. reported that the number of pericyte ghosts increased after eight months of diabetes [22]. Thus, a limitation of the present study was that it is difficult to separate pericytes from endothelial cells. Cell ratio changes observed in the capillaries of diabetic rats could be the result of changes in endothelial cells, pericytes, or both.

AGEs are the adducts of sugar aldehyde groups and amino nucleophiles in proteins that form an Amadori product in a process termed protein glycation [23]. A previous study reported that AGEs play a role in DR by inducing apoptosis and inflammation in retinal pericytes via interaction with a receptor for AGE (RAGE) [24]. This process can upregulate the pro-apoptotic gene, Bax, to promote development of apoptosis in bovine retinal capillary pericytes [25]. Interaction of AGEs and RAGE activates nuclear factor- $\kappa$ B (NF- $\kappa$ B) and generates pro-inflammatory cytokines, such as IL-1 $\beta$ , IL-6, and TNF- $\alpha$  [26]. The present study demonstrated increased levels of AGEs in diabetic rats, suggesting that they are responsible for retinal pericyte apoptosis. This result was similar to results by Kim et al. [27]. Anti-apoptotic effects of AST are probably due

to its inhibitory effects on production of AGEs in the retina.

Chronic inflammation plays a key role in progression of DR and exacerbates DR deterioration [8]. Pro-inflammatory cytokines can be activated by ischaemia-reperfusion injury and interaction of AGEs and RAGE [28]. Apoptosis of pericytes has been reported to be associated with inflammation [19]. Additionally, pro-inflammatory cytokines (IL-6 and TNF- $\alpha$ ) in the retinal vessels can activate pro-apoptosis signalling pathways and promote apoptosis of retinal capillary cells [29]. A study by Kowluru et al. demonstrated the importance of inflammation in retinal pericyte apoptosis by detecting pro-inflammatory cytokines *in vitro* [30]. Izumi-Nagai et al. and Suzuki et al. reported that AST could inhibit NF- $\kappa$ B activation and downregulate inflammatory cytokines in mice with choroidal neovascularization and uveitis [15, 16]. Park et al. confirmed that AST could reduce inflammatory cytokines and C-reactive protein in plasma, enhancing the cytotoxic activity of natural killer cells and enhancing the immune response in young healthy women [17]. Another study reported that AST reduced NF- $\kappa$ B-mediated inflammation in high-fructose and high-fat diet-fed mice [31]. Previously, anti-inflammatory mechanisms of AST have been reported both *in vitro* and *in vivo*. AST reduced the release of inflammatory factors, including IL-6 and TNF- $\alpha$ , as detected using ELISA and Western blot, in a model of hepatic ischaemia reperfusion [32]. Pro-inflammatory cytokines, such as TNF- $\alpha$ , can promote the activation of caspase-3, which can induce apoptosis in retinal endothelial cells [33]. In the present study, it was observed that AST could decrease levels of IL-6, TNF- $\alpha$ , and caspase-3 in the DM+AST group at both protein and mRNA levels, compared to levels in the DM group. This suggests that AST can inhibit development of DR and apoptosis of retinal pericytes by reducing levels of pro-inflammatory cytokines. Present data showed that these indices were upregulated in all diabetic rats, highlighting the relationship between pericyte apoptosis and inflammation.

However, whether AST affects pericyte apoptosis by inhibiting both AGE formation and inflammation or only inhibiting AGE formation remains uncertain. Another limitation of this study was that only a single dose of AST (20 mg/kg/day)

was used, based on previous findings. It would be of interest to conduct a dose-response to identify the optimal dose of AST for treatment of STZ-induced diabetic rats. AST could not prevent the destruction of pancreatic  $\beta$  cells induced by STZ in the type 1 diabetes model, as indicated by its inability to prevent hyperglycaemia in the rats. Despite this limitation, AST was still able to afford retinal protection. Protective effects of AST in type 2 diabetes models could be even greater and are of interest. These issues will be addressed in future studies.

### Conclusion

The present study demonstrated that administration of AST to STZ-induced diabetic rats partially ameliorated adverse retinal changes that occurred in diabetic rats. These structural changes were likely the result of reduced AGE production, pericyte apoptosis, and inflammation. Although AST could not prevent rises in blood glucose induced by STZ, its ability to protect the eye, at least partially, from the ravages of diabetes suggests that it holds great promise as a therapeutic agent in diabetic patients.

### Disclosure of conflict of interest

None.

### Abbreviations

DR, diabetic retinopathy; BRB, blood-retina barrier; AGE, advanced glycation end product; AST, astaxanthin; STZ, streptozotocin; IL-6, interleukin-6; TNF- $\alpha$ , tumour necrosis factor- $\alpha$ ; NF- $\kappa$ B, nuclear factor- $\kappa$ B; E/P, endothelial cell to pericyte ratio; PBS, phosphate-buffered saline; DAB, 3,3'-diaminobenzidine; SD, standard deviation; RAGE, advanced glycation end-product receptor; IOD, integrated optical density.

**Address correspondence to:** Zhijun Wang, Department of Ophthalmology, China-Japan Friendship Hospital, Chaoyang District, Beijing, China. E-mail: wangzhijuncj@sina.com

### References

- [1] Runkle EA, Antonetti DA. The blood-retinal barrier: structure and functional significance. *Methods Mol Biol* 2011; 686: 133-148.
- [2] Thomas RL, Dunstan F, Luzio SD, Roy Chowdury S, Hale SL, North RV, Gibbins RL, Owens DR. Incidence of diabetic retinopathy in people

## Astaxanthin against diabetic retinal vessels and inflammatory

- with type 2 diabetes mellitus attending the diabetic retinopathy screening service for wales: retrospective analysis. *BMJ* 2012; 344: e874.
- [3] Ortiz G, Salica JP, Chuluyan EH, Gallo JE. Diabetic retinopathy: could the alpha-1 antitrypsin be a therapeutic option? *Biol Res* 2014; 47: 58.
- [4] Zang J, Guan G. Study of pigment epithelium-derived factor in pathogenesis of diabetic retinopathy. *Eye Sci* 2015; 30: 81-88.
- [5] Shin ES, Sorenson CM, Sheibani N. Diabetes and retinal vascular dysfunction. *J Ophthalmic Vis Res* 2014; 9: 362-373.
- [6] Hammes HP. Pericytes and the pathogenesis of diabetic retinopathy. *Horm Metab Res* 2005; 37 Suppl 1: 39-43.
- [7] Yamagishi S, Ueda S, Matsui T, Nakamura K, Okuda S. Role of advanced glycation end products (AGEs) and oxidative stress in diabetic retinopathy. *Curr Pharm Des* 2008; 14: 962-968.
- [8] Park YG, Roh YJ. New diagnostic and therapeutic approaches for preventing the progression of diabetic retinopathy. *J Diabetes Res* 2016; 2016: 1753584.
- [9] Fassett RG, Coombes JS. Astaxanthin, oxidative stress, inflammation and cardiovascular disease. *Future Cardiol* 2009; 5: 333-342.
- [10] Pashkow FJ, Watumull DG, Campbell CL. Astaxanthin: a novel potential treatment for oxidative stress and inflammation in cardiovascular disease. *Am J Cardiol* 2008; 101: 58D-68D.
- [11] Ikeuchi M, Koyama T, Takahashi J, Yazawa K. Effects of astaxanthin in obese mice fed a high-fat diet. *Biosci Biotechnol Biochem* 2007; 71: 893-899.
- [12] Kim YJ, Kim YA, Yokozawa T. Protection against oxidative stress, inflammation, and apoptosis of high-glucose-exposed proximal tubular epithelial cells by astaxanthin. *J Agric Food Chem* 2009; 57: 8793-8797.
- [13] Dong LY, Jin J, Lu G, Kang XL. Astaxanthin attenuates the apoptosis of retinal ganglion cells in db/db mice by inhibition of oxidative stress. *Mar Drugs* 2013; 11: 960-974.
- [14] Chitwood LA. Tube dilution antimicrobial susceptibility testing: efficacy of a microtechnique applicable to diagnostic laboratories. *Appl Microbiol* 1969; 17: 707-709.
- [15] Yeh PT, Huang HW, Yang CM, Yang WS, Yang CH. Astaxanthin inhibits expression of retinal oxidative stress and inflammatory mediators in streptozotocin-induced diabetic rats. *PLoS One* 2016; 11: e0146438.
- [16] Chan KC, Pen PJ, Yin MC. Anticoagulatory and antiinflammatory effects of astaxanthin in diabetic rats. *J Food Sci* 2012; 77: H76-80.
- [17] Klaassen I, Van Noorden CJ, Schlingemann RO. Molecular basis of the inner blood-retinal barrier and its breakdown in diabetic macular edema and other pathological conditions. *Prog Retin Eye Res* 2013; 34: 19-48.
- [18] Mizutani M, Kern TS, Lorenzi M. Accelerated death of retinal microvascular cells in human and experimental diabetic retinopathy. *J Clin Invest* 1996; 97: 2883-2890.
- [19] Barber AJ, Gardner TW, Abcouwer SF. The significance of vascular and neural apoptosis to the pathology of diabetic retinopathy. *Invest Ophthalmol Vis Sci* 2011; 52: 1156-1163.
- [20] Beltramo E, Berrone E, Giunti S, Gruden G, Perin PC, Porta M. Effects of mechanical stress and high glucose on pericyte proliferation, apoptosis and contractile phenotype. *Exp Eye Res* 2006; 83: 989-994.
- [21] Kowluru RA. Diabetic retinopathy: mitochondrial dysfunction and retinal capillary cell death. *Antioxid Redox Signal* 2005; 7: 1581-1587.
- [22] Robison WG Jr, McCaleb ML, Feld LG, Michaelis OE 4th, Laver N, Mercandetti M. Degenerated intramural pericytes ('ghost cells') in the retinal capillaries of diabetic rats. *Curr Eye Res* 1991; 10: 339-350.
- [23] Chen M, Curtis TM, Stitt AW. Advanced glycation end products and diabetic retinopathy. *Curr Med Chem* 2013; 20: 3234-3240.
- [24] Maeda S, Matsui T, Ojima A, Takeuchi M, Yamagishi S. Sulforaphane inhibits advanced glycation end product-induced pericyte damage by reducing expression of receptor for advanced glycation end products. *Nutr Res* 2014; 34: 807-813.
- [25] Chen BH, Jiang DY, Tang LS. Advanced glycation end products induce apoptosis and expression of apoptotic genes in cultured bovine retinal capillary pericytes. *Zhonghua Yan Ke Zhi* 2003; 39: 224-227.
- [26] Neumann A, Schinzel R, Palm D, Riederer P, Munch G. High molecular weight hyaluronic acid inhibits advanced glycation endproduct-induced NF-kappaB activation and cytokine expression. *FEBS Lett* 1999; 453: 283-287.
- [27] Kim J, Jo K, Lee IS, Kim CS, Kim JS. The extract of aster koraiensis prevents retinal pericyte apoptosis in diabetic rats and its active compound, chlorogenic acid inhibits AGE formation and AGE/RAGE interaction. *Nutrients* 2016; 8.
- [28] Singh VP, Bali A, Singh N, Jaggi AS. Advanced glycation end products and diabetic complications. *Korean J Physiol Pharmacol* 2014; 18: 1-14.
- [29] Nahomi RB, Palmer A, Green KM, Fort PE, Nagaraj RH. Pro-inflammatory cytokines downregulate Hsp27 and cause apoptosis of human retinal capillary endothelial cells. *Biochim Biophys Acta* 2014; 1842: 164-174.
- [30] Kowluru RA, Zhong Q, Kanwar M. Metabolic memory and diabetic retinopathy: role of in-

## Astaxanthin against diabetic retinal vessels and inflammatory

- flammatory mediators in retinal pericytes. *Exp Eye Res* 2010; 90: 617-623.
- [31] Bhuvaneswari S, Yogalakshmi B, Sreeja S, Anuradha CV. Astaxanthin reduces hepatic endoplasmic reticulum stress and nuclear factor-kappaB-mediated inflammation in high fructose and high fat diet-fed mice. *Cell Stress Chaperones* 2014; 19: 183-191.
- [32] Li J, Wang F, Xia Y, Dai W, Chen K, Li S, Liu T, Zheng Y, Wang J, Lu W, Zhou Y, Yin Q, Lu J, Zhou Y, Guo C. Astaxanthin pretreatment attenuates hepatic ischemia reperfusion-induced apoptosis and autophagy via the ROS/MAPK pathway in mice. *Mar Drugs* 2015; 13: 3368-3387.
- [33] Blocksom JM, Huang J, Kerkar S, Hinshaw C, Williams M, Tyburski JG, Carlin AM, Steffes CP, Wilson RF. Endothelial cells protect against lipopolysaccharide-induced caspase-3-mediated pericyte apoptosis in a coculture system. *Surgery* 2004; 136: 317-322.